Electronic Supplementary Material (ESI) for Sustainable Energy & Fuels.

Supporting information

Predictable Interfacial Mass Transfer Intensification of Sn-N doped multichannel hollow carbon nanofibers for CO_2 electro-reduction reaction

Ziqiang Cao,[a, ‡] *Song Liu,*[b, ‡] *Keyi Xu,*[a] *Yuanxin Mao,*[c] *Yingjie Wu,*[d] *Qing Mao*[a,*]

1. Experimental section

1.1 Chemical and materials

Polyacrylonitrile (PAN, Mw=150000) was from Sigma-Aldrich. Polymethyl methacrylate (PMMA, Mw=120000) and Tin (IV) chloride pentahydrate ($SnCl_4·5H_2O$, AR, 98%) were purchased from Macklin. Potassium bicarbonate ($KHCO_3$, AR, 99.5%), hydrochloric acid (HCl, AR, 36-38%), Isopropyl alcohol (AR, ≥99.7%) and N, N-dimethy iformamide (DMF, AR, ≥99.5%) were purchased from Kermel. Nafion® D520 solution (5 wt. %) and Nafion® 115 membrane were from Dupont. The hydrophobic carbon paper (TGP-H-060) was from Japan Toray Company. Deionized Water was obtained by the Synergy Water Purification System (Millipore, >18Ω).

1.2 Synthesis of Sn and N co-doped carbon nanofibers

In a typical synthesis of Sn and N co-doped carbon nanofibers (Sn/N-CNF), a mixture of polyacrylonitrile (PAN, 0.67 g), polymethyl methacrylate (PMMA, 0.67 g), and Tin (IV) chloride pentahydrate ($SnCl_4$, 0.70 g) were first dissolved into 10 mL N, N-dimethylformamide. Then, the mixture was stirred vigorously at 60°C for 12 hours to form a transparent viscous solution. Subsequently, the solution was loaded into a syringe with a steel nozzle (internal diameter of 0.67

mm) and then the electrospinning was conducted under the following conditions: a feeding rate of 0.5 $mL\cdot h^{-1}$, a tip-to-collector distance of 15 cm and a high voltage of 12.5 kV. The obtained electrospun fibers successively underwent a two-stage pre-oxidization and carbonization process. First stage: The fibers were firstly stabilized at 250℃ for 10 minutes with an air flow of 5 $mL\cdot min^{-1}$, and then pre-oxidized with an increasing temperature with different ramping rates (2℃/min, 5℃/min, 10℃/min, respectively). The pre-oxidized temperature was determined by the thermo gravimetric (STA) experiments (Fig. S1a). As the temperature reach 380 ℃, annealing is carried out for all samples. Second stage: the pre-oxidized fibers were pyrolyzed again in an atmosphere of H_2-Ar mixture (2 vol. % H_2) for 3 hours at 1000℃. After cooling down to room temperature, the samples were grinded to powder in an agate mortar, and then leached at 80 ℃ in 3 mol L^{-1} HCl for 96 hours to remove metal particles and unstable species. After washing with DI. water for 5 times and dried at 80 ℃ in an oven for 24 hours, the Sn/N-CNFs with hollow multichannel are obtained. Sn/N-CNFs without additional PMMA were also prepared using the same synthesis processes. The synthesis details are shown in Fig. 1.

1.3 Preparation of gas diffusion electrode (GDE)

Catalytst inks for CO_2RR GDE preparation is synthesized by mixing 10 mg as-prepared catalysts with 480 μL isopropanol (AR), 480 μL deionized water and 40 μL Nafion solution (5 wt. %). Ultrasonic dispersed the ink in an ice water for 40 minutes. And then, brushed it onto a Toray carbon paper piece with an effect geometric area of 1.0 cm^2. The catalyst loading was 1.0 mg cm^{-2}.

1.4 Techniques for Characterization

Pyrolysis process for the electrospun fibers was analyzed through a simultaneous thermal analyzer (STA, TGA/DSC3+, METTLER TOLEDO). The morphology, elements mapping and crystal structure of Sn/N-CNFs were observed by field emission scanning electron microscopy (FESEM, NOVA Nano SEM 450, FEI), transmission electron microscopy (TEM, Tecnai G2 F30 S-Twin, Thermo Scientific) and X-ray diffraction (XRD, D/Max 2400, Smartlab), respectively. The scanning rate and scanning range for the XRD test were 5° min^{-1} and 10-80°, respectively. The catalysts surface valence states were obtained using X-ray photoelectron spectroscopy analysis (XPS, ESCALAB 250Xi, Thermo Scientific), in which the adventitious carbon (C 1s) at the binding energy (BE) of 284.8 eV was taken as the reference. Sn loading in the catalysts inside was quantified by inductively coupled plasma emission spectrometer (ICP-OES, IRIS Intrepid II

XPS, Thermal Scientific). Pore structure and specific surface area of the Sn/N-CNFs were analyzed by N_2 adsorption (ASAP 2020, American Mike) at 77.3 K. Meanwhile, the CO_2 physical adsorption experiments were conducted using Quadrasorb S (Quantachrome Instruments U.S.) at 273.15 K.

1.5 Electrochemical performance

All electrochemical characterizations were tested using an electrochemical workstation (Reference 3000, Gamry) in a H-type cell, that separated by a cation-exchange membrane (Nafion®115) in 0.5 mol L^{-1} $KHCO_3$ solution. As-prepared GDEs, platinum foil and saturated calomel electrode (SCE) were taken as the working electrodes, counter electrode and reference electrode, respectively. Before CO_2RR performance test, the cathode chamber of the H-type cell was filled with gas mixture of CO_2 (99 %, vol.%) and Ar (1 %, vol.%) for 20 minutes. CO_2RR performance was evaluated in the potentiostatic mode, in which each potential was held for 1800 s to obtain static polarization and stable products. During the test, the flow rate of the CO_2-Ar mixture was 40 mL min^{-1} and the temperature was 25°C. CO_2RR products were detected by gas chromatography (7890 B, Agilent) with a flame ionization detector (FID) and two thermal conductivity detectors (TCD). In order to obtain the content of the product more accurately, the internal standard method is adopted during the GC detecting process, in which, Ar (1%) is used as the internal standard. The internal resistance was measured by electrochemical impedance spectroscopy (EIS) at DC offset of -1.6 V (vs. SCE), AC amplitude of 10 mV, in the frequency domain range from 100 kHz to 0.1 Hz. Electrochemical surface areas (ECSA) of the CO_2RR catalysts was qualitatively evaluated by calculating the double-layer capacitance (C_{dl}), and the cyclic voltammetry (CV) was conducted to evaluate the apparent electrochemical C_{dl}. The scan rates of CV measurements were 1,10, 20, 40, 60, 80 and 100 mV s^{-1}, respectively, and the potential was ranged from 50 to 150 mV (vs. SCE). The C_{dl} is estimated by linear fitting the plot of $\Delta j = j_a - j_c$ (j_a and j_c are the anodic and cathodic current densities, respectively) at 100 mV (vs. SCE) against the scan rates.

1.6 Kinetics calculation section of CO_2RR to CO

The kinetics parameters of the kinetic models were obtained by fitting the models with steady-state internal resistance (IR) corrected J_{CO}-V curves by a global optimization method, which composes of a random search using genetic algorithm and a local optimization employing trustregion-reflective algorithm. All simulations were performed using a commercial software package (MATLAB R2010b, the MathWorks Inc.).

Assuming the single Sn atom is the active site in CO_2RR, the enrolled reaction rate equations and the control equations are listed in Table S1. Corresponding kinetics parameters under 0.55 mA site^{-1} 10^{-17} are listed in Table S2, Where K is the reaction rate constant (mol m^{-2} s^{-1}), η is the overpotential (V), R is the gas constant (J mol^{-1} K^{-1}), T is the temperature (K). It is suggesting that the step Eq (2) is the rate determine step (RDS.) of CO_2RR to CO on SnN-HF-5 and SnN-F.

2. Supplementary Figures and Tables

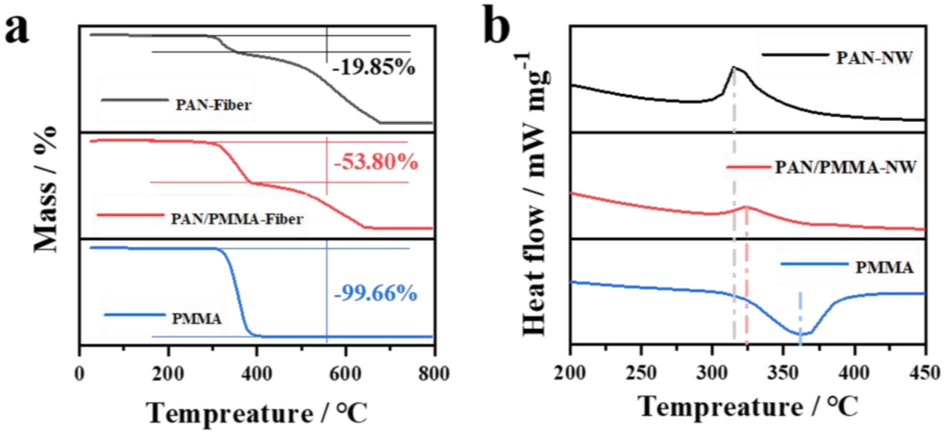

Figure S1. (a) Thermogravimetric analysis (TGA) curves and (b) differential scanning calorimeter (DSC) curves of PAN fiber, PAN/PMMA fiber and PMMA at air. The heating rate was 10°C/min. PMMA was completely decomposed at 380°C.

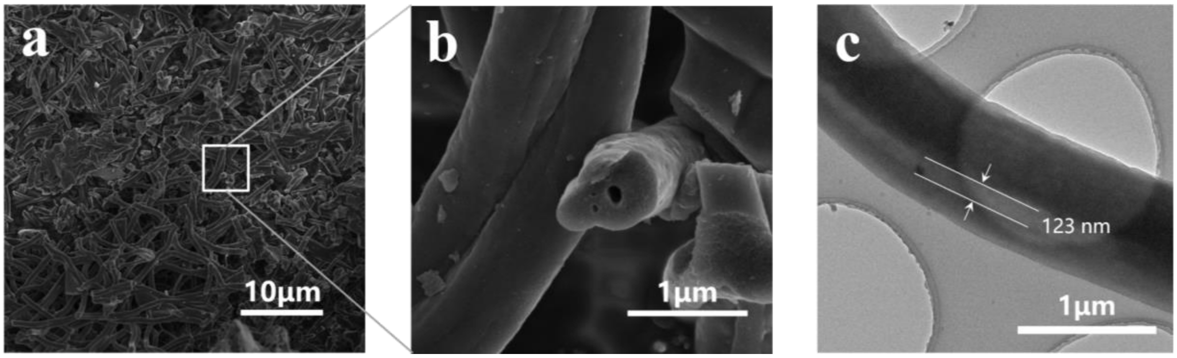

Figure S2. (a, b) FESEM and (c) TEM images of SnN-HF-2.

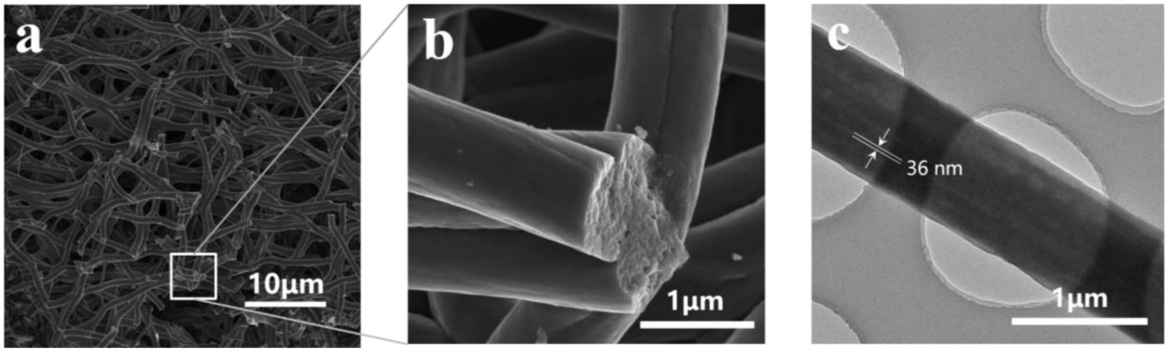

Figure S3. (a, b) FESEM and (c) TEM images of SnN-HF-10.

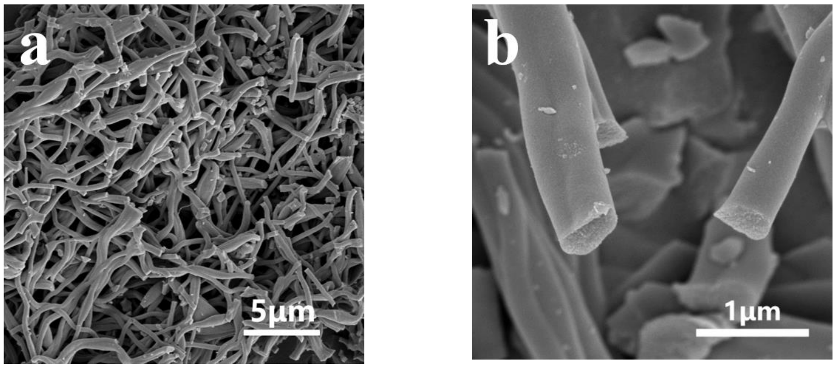

Figure S4. (a, b) FESEM images of SnN-F.

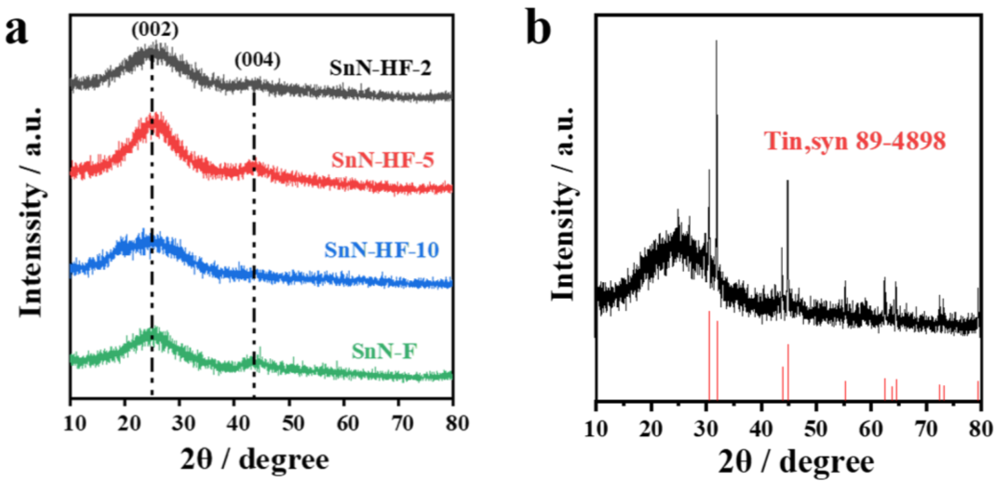

Figure S5. XRD patents of (a) Sn/N-CNFs and (b) SnN-HF-5 before leaching in HCl. (Tin, syn 89-4898 from XRD standard PDF).

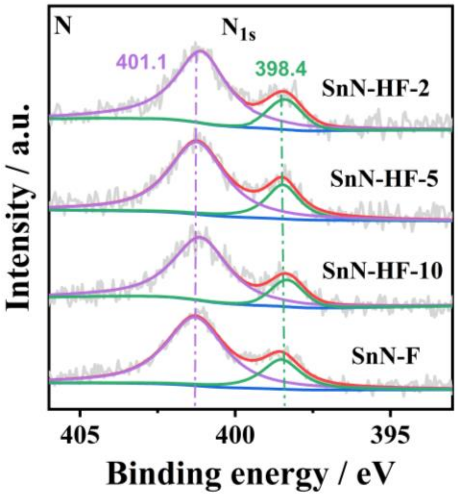

Figure S6. N 1s XPS spectra of Sn/N-CNFs.

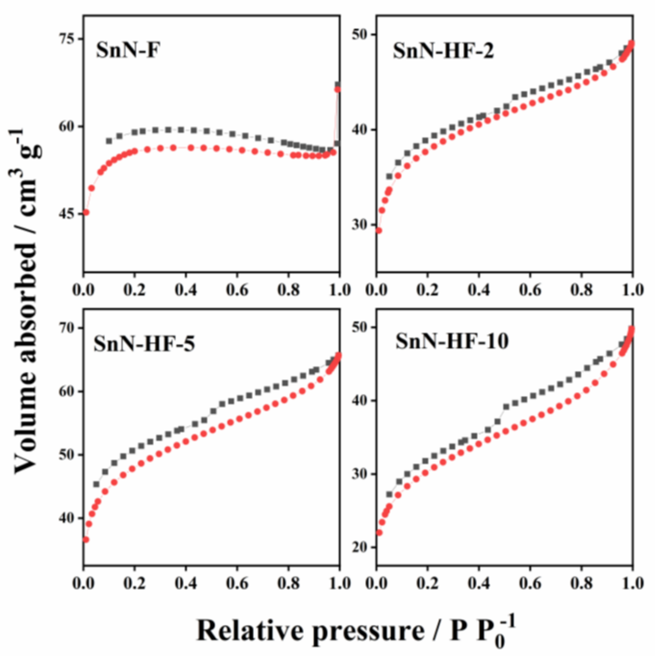

Figure S7. N_2 isothermal adsorption and desorption curve of Sn/N-CNFs.

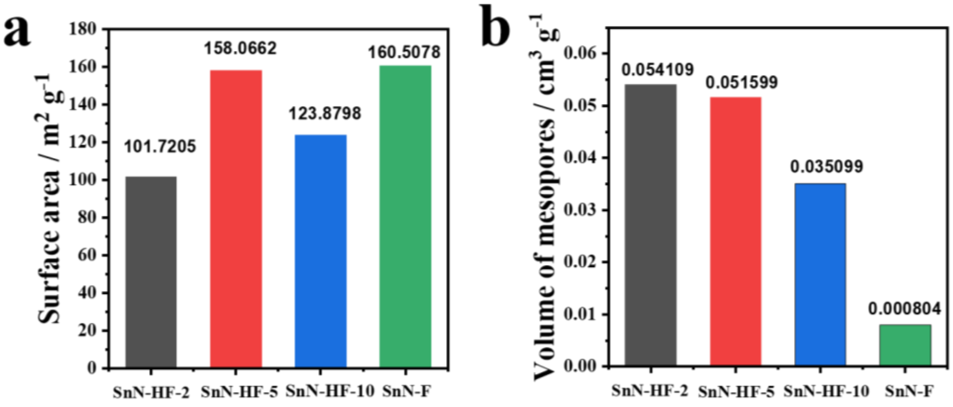

Figure S8. Results of N_2-BET surface area (a) and mesopore volumes (b) of Sn/N-CNFs.

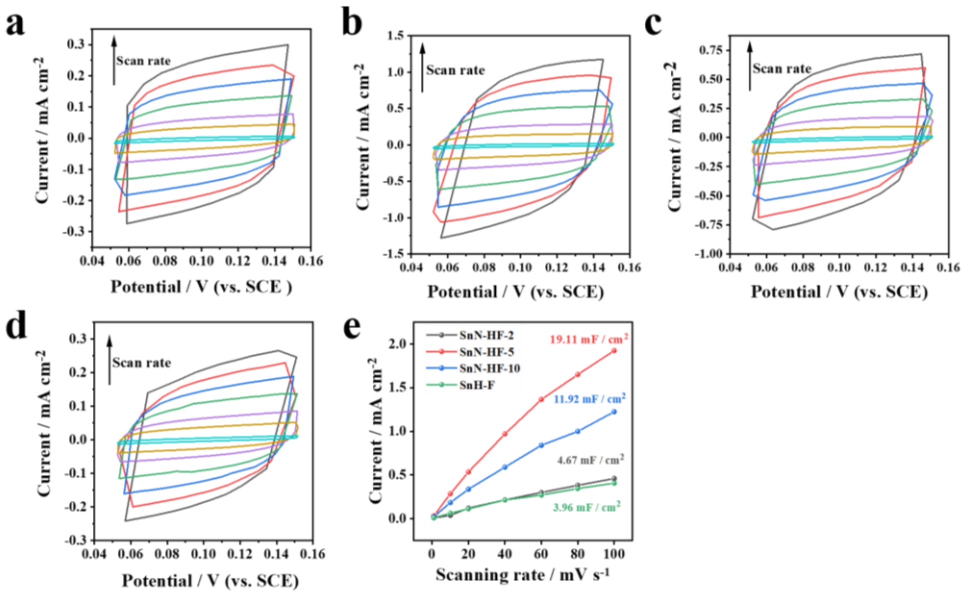

Figure S9. Cyclic voltammetry curves of Sn/N-CNFs between 50 mV (vs. SCE) to 150 mV (vs. SCE) in CO_2 saturated 0.5 M $KHCO_3$ solution at different scanning speeds of 1,10, 20, 40, 60, 80, 100 / mV s^{-1}. (a) SnN-HF-2, (b) SnN-HF-5, (c) SnN-HF-10 and (d) SnN-F. (e) Calculation results of electric double layer capacitor (C_{dl}).

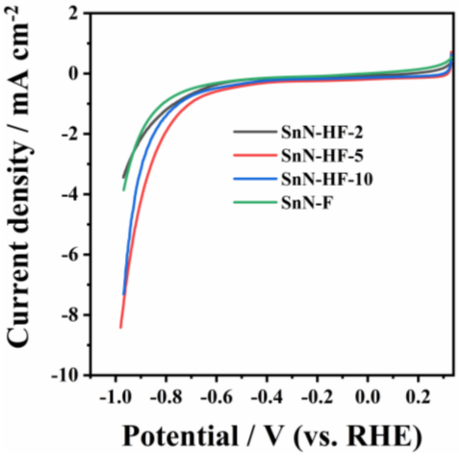

Figure S10. CO_2RR performance on the Sn/N-CNFs measured by linear sweep voltammetry (LSV, in CO_2-saturated electrolytes, the scanning rare is 10 mV s^{-1}).

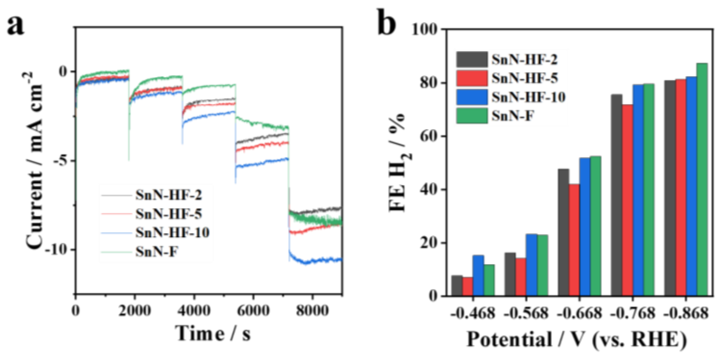

Figure S11. (a) Potentiostatic test results at different applied potentials and (b) comparison of H_2 Faraday efficiency of Sn/N-CNFs.

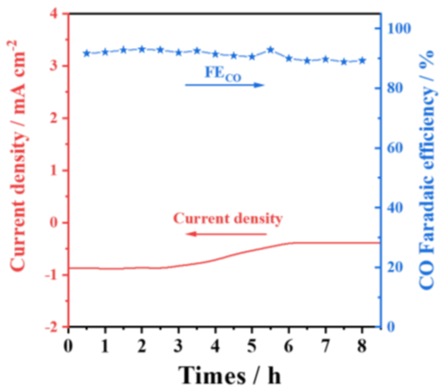

Figure S12. CO_2RR stability at -0.468 V (vs. RHE) of the SnN-HF-5

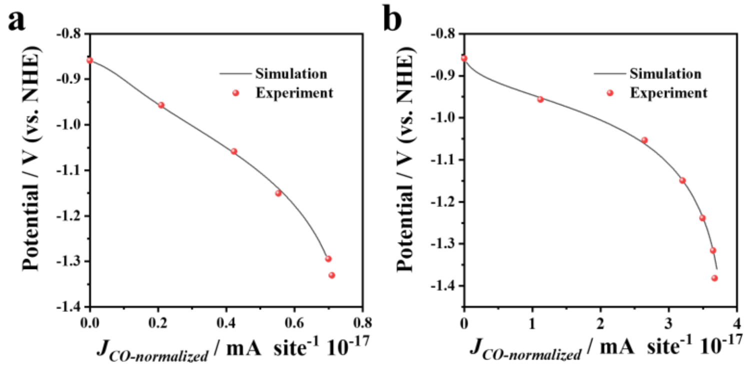

Figure S13. The CO-partial J-V simulation and experiment curve of (a) SnN-HF-5 and (b) SnN-HF.

Table S1. Reaction rate equations (EqS. 1-6) and control equations (EqS. 7-9) for CO_2 reduction to CO taking place on SnN-HF-5 and SnN-F.

$$r_1 = K_{101} \cdot \left(1 - \theta_{CO_2,\,ads} - \theta_{COOH,\,ads}\right) \cdot \left(\frac{P_{CO_2}}{P^{\Theta}}\right) \tag{EqS. 1}$$

$$r_{\text{-}1} = K_{102} \cdot \theta_{CO_2,ads} \tag{EqS. 2}$$

$$r_2 = K_{201} \cdot \theta_{CO_2,ads} \cdot \left(\frac{c_{CO_2}}{c^{\Theta}}\right) \cdot \exp\left(\frac{\alpha F \eta}{RT}\right) \tag{EqS. 3}$$

$$r_{\text{-}2} = K_{201} \cdot \theta_{COOH_{ads}} \cdot \left(\frac{c_{HCO_3^-}}{c^{\Theta}}\right) \cdot \exp\left(-\frac{(1-\alpha) F \eta}{RT}\right) \tag{EqS. 4}$$

$$r_3 = K_{301} \cdot \theta_{COOH_{ads}} \cdot \left(\frac{c_{CO_2}}{c^{\Theta}}\right) \cdot \exp\left(\frac{\alpha F \eta}{RT}\right) \tag{EqS. 5}$$

$$r_{\text{-}3} = K_{301} \cdot \left(1 - \theta_{CO_{2,ads}} - \theta_{COOH_{ads}}\right) \cdot \left(\frac{P_{CO}}{P^{\Theta}}\right) \cdot \left(\frac{c_{HCO_3^-}}{c^{\Theta}}\right) \cdot \exp\left(-\frac{(1-\alpha) F \eta}{RT}\right) \tag{EqS. 6}$$

$$C_{CO_2} \frac{d\theta_{CO_2}}{dt} = r_1 - r_{-1} - r_2 + r_{\text{-}2} \tag{EqS. 7}$$

$$C_{COOH} \frac{d\theta_{COOH}}{dt} = r_2 - r_{-2} - r_3 + r_{\text{-}3} \tag{EqS. 8}$$

$$C_{dl} \frac{dE}{dt} = j(t) - \left[\left(r_2 - r_{-2}\right) + \left(r_3 - r_{-3}\right)\right] \cdot F / n \tag{EqS. 9}$$

Note: Where r is the elementary reaction rate (mol m^{-2} s^{-1}), K is the reaction rate constant (mol m^{-2} s^{-1}), c is the concentration (mol m^{-3}), θ is the coverage, α is the symmetry coefficient, η is the overpotential (V), R is the gas constant (J mol^{-1} K^{-1}), T is the temperature (K), θ which subscripts CO_2 and COOH represent the intermediate $CO_{2,\,ads}$ and $COOH_{,\,ads}$, respectively, and c which subscripts CO_2 and HCO_3^- represent the reactant CO_2 and electrolyte $KHCO_3$, respectively.

Table S2. The rate constants under 0.55 mA site^{-1} 10^{-17} of the electrochemical elementary steps of CO2RR on SnN-HF-5 and SnN-F.

Reaction rate constant	**SnN-HF-5 (mol·s^{-1}·m^{-2})**	**SnN-F (mol·s^{-1}·m^{-2})**
K_{101}	2.76×10^{4}	4.67×10^{3}
K_{201}	7.00×10^{5}	4.84×10^{7}
$K_{201} \cdot \exp\left(\frac{\alpha F \eta}{RT}\right)$	4.01	2.68×10^{3}
$K_{202} \cdot \exp\left(-\frac{(1-\alpha) F \eta}{RT}\right)$	3.36×10^{-1}	3.19×10^{-3}
$K_{301} \times \exp\left(\frac{\alpha F \eta}{RT}\right)$	7.45	1.58×10^{4}
$K_{302} \cdot \exp\left(-\frac{(1-\alpha) F \eta}{RT}\right)$	1.87×10^{-4}	3.31×10^{-3}

Table S3. The proportion of tin of different valence states deconvoluted by Sn 3d XPS spectrum.

Sample	**Sn^{2+} percentage (%)**	**Sn^{4+} percentage (%)**
SnN-HF-2	17.32	82.68
SnN-HF-5	16.93	83.07
SnN-HF-10	17.66	82.34
SnN-F	18.75	81.25

Table S4. The proportion of different N species deconvoluted by N 1s XPS spectrum.

Sample	**Pyridine-N Percentage (%)**	**Quaternary-N Percentage (%)**
SnN-HF-2	25.15	74.85
SnN-HF-5	28.13	71.87
SnN-HF-10	27.21	72.79
SnN-F	28.32	71.68

Table S5. Sn contents of Sn/N-CNFs obtained by inductively coupled plasma emission spectrometer (ICP-OES).

Sample	**SnN-HF-2**	**SnN-HF-5**	**SnN-HF-10**	**SnN-F**
Sn Contents (%)	0.691	0.689	0.959	2.110